

ELECTRONIC STRUCTURE OF POLYMORPHISMS PHASES OF LEAD-FREE FERROELECTRIC $\text{Bi}_{0.5}\text{Na}_{0.5}\text{TiO}_3$ MATERIALS

Vu Tien Lam¹, Nguyen Hoang Thoan¹, Nguyen Ngoc Trung¹, Dang Duc Dung¹
Duong Quoc Van²

Received: 08 November 2021/ Accepted: 25 March 2022/ Published: April 2022

Abstract: *Bismuth-based ferroelectric ceramics are currently under intense investigation for the potential as Pb-free alternatives to lead zirconate titanate-based ($\text{Pb}(\text{Zr},\text{Ti})\text{O}_3$ -based) piezoelectrics. In this work, first-principle calculations were performed for the electronic structures of sodium bismuth titanate ($\text{Bi}_{0.5}\text{Na}_{0.5}\text{TiO}_3$) materials with all possible crystal symmetries, including rhombohedral, monoclinic, tetragonal, and rhombohedral. We expected that our works could help further understand the role of phase transition in lead-free ferroelectric $\text{Bi}_{0.5}\text{Na}_{0.5}\text{TiO}_3$ materials.*

Keywords: $\text{Bi}_{0.5}\text{Na}_{0.5}\text{TiO}_3$, Lead-free ferroelectric, First principle calculation.

1. Introduction

Lead-based ferroelectric $\text{Pb}(\text{Zr},\text{Ti})\text{O}_3$ materials have been given much attention because their piezoelectric, ferroelectric, and dielectric properties are better than lead-free ferroelectric materials. With the rapid industrial development, the amounts of Pb used in electronic devices have increased, seriously affecting the environment and human health. Thus, the performance of eco-friendly lead-free ferroelectric materials, such as $\text{Bi}_{0.5}\text{Na}_{0.5}\text{TiO}_3$, should be improved [1]. Sodium bismuth titanate BNT materials, first fabricated by Smolensky et al. in 1960 [2], are ferroelectric materials with Curie temperature of 320°C , remanent polarization of $38 \mu\text{C}/\text{cm}^2$, and coercive field of $73 \text{ kV}/\text{cm}$ at room temperature [2] [3]. $\text{Bi}_{0.5}\text{Na}_{0.5}\text{TiO}_3$ materials have a low piezoelectric coefficient of $\sim 70\text{-}80 \text{ pC}/\text{N}$ due to their high coercive field [3]. $\text{Bi}_{0.5}\text{Na}_{0.5}\text{TiO}_3$ materials exhibited rhombohedral structure at room temperature and monoclinic symmetry [4] [5]. Pronin et al. [6] obtained that the first phase transition tetragonal-cubic phase occurred at 320°C , whereas the second phase transition temperature of the rhombohedral-tetragonal phase was 540°C as they determined the Curie temperature. The average symmetries of rhombohedral, monoclinic, and cubic BNT structures are $R3c$, Cc , $P4bm$, and $Fm-3m$ space groups, respectively.

Recently, optical bandgap, diffuse scattering, infrared, and high-pressure Raman spectra of BNT have been extensively studied experimentally [7-10]. The crystal structure of $\text{Bi}_{0.5}\text{Na}_{0.5}\text{TiO}_3$ materials was determined by neutron powder diffraction at 698 K [7]. In the theoretical aspect, first-principle calculations were widely adopted to study the

¹Multifunctional Ferroics Materials Lab, School of Engineering Physics, Ha Noi University of Science and Technology; Email: dung.dangduc@hust.edu.vn

² Faculty of Physics, Ha Noi National University of Education

structure, band structure, and electronic properties of perovskite ferroelectric materials, including BNT [11]. BNT with a high-temperature cubic phase is a semiconductor, discovered by Xu and Ching [12]. Bujakiewicz-Koronska and Natazon investigated the elastic properties of BNT crystals [13]. Gröting et. al. [14] calculated the phase stability of BNT under pressure using ab-initio supercell calculations, and Niranjana et. al. [15] investigated the dielectric properties and phonon frequencies for the rhombohedral crystal structure by density functional perturbation theory. Most theoretical studies on BNT focused on rhombohedral and cubic phases, while only a few works were conducted on tetragonal and monoclinic phases. Tetragonal and monoclinic phases are transitional between the rhombohedral and cubic ones of BNT, and they are often related to the interplaying between different phases [16]; it would be beneficial to study all the four phases of BNT under the same approach to provide comprehensive perspective. In this work, we have performed first-principle calculations on BNT for all four phases possible.

2. Experiments

In this work, all DFT calculations were performed using the Cambridge Serial Total Energy Package (CASTEP) module in the Materials Studio software. For exchange-correlation energy, we adopted the generalized gradient approximation (GGA) using Perdew - Burke - Ernzerhof (PBE) exchange-correlation functionals [16], which is sufficiently accurate to describe the crystal structures and electronic properties of perovskite compounds [17]. The energy cutoff of the plane-wave basis functions was set to be 500 eV, which yields sufficiently convergence of the total energy differences better than 10^{-6} eV per atom. The Monkhorst-Pack scheme was used to sample the Brillouin zone; and the k-point sampling method [18] was chosen for the reciprocal space integrations over the Brillouin zone with good convergence for the calculated properties, where the k-point mesh of $5 \times 5 \times 4$ is used. The structures were fully relaxed with convenient primary cells. Four BNT phases, including rhombohedral, monoclinic, tetragonal, and cubic, were simulated using $R3c$, Cc , $P4bm$, and $Fm-3m$ space groups, respectively. The cubic and rhombohedral BNT structures were assumed from the experimental lattice parameters [19].

3. Results and Discussion

3.1. Crystal structures

Fig.1 shows four different crystal structures of BNT. Adopting of an ordered structure facilitates the calculations and helps avoid computational artifacts [20]. The replacement of Na and Bi atoms at A-sites leads to lower, the symmetries of the rhombohedral, monoclinic, tetragonal, and cubic BNT phases to $R3c$, Cc , $P4bm$, $Fm-3m$, respectively. At room temperature, the optimized lattice constants for the conventional cell of the rhombohedral phase are $a = 5.501 \text{ \AA}$ and $c = 13.496 \text{ \AA}$, which are close to the experimental value of 5.488 \AA and 13.504 \AA [19]. Meanwhile, at a higher temperature, the lattice constants of monoclinic, tetragonal, and cubic phases have been optimized close to the experimental values, respectively. Table 1 presents the optimized lattice constants of the four BNT phases in comparison to the experimental values by G. O. Jones [7], H. Lü [19] and E. Aksel [21] (within 1%-2%).

Table 1. Optimized calculated and experimental lattice parameters (\AA) and atomic coordinates in four BNT phases

Rhombohedral phase		
	<i>Calc.</i>	<i>Ref. [19]</i>
<i>a</i>	5.501	5.488
<i>c</i>	13.496	13.504
α	90°	90°
γ	120°	120°
Na	(0 0 0.259)	(0 0 0.257)
Bi	(0 0 0.783)	(0 0 0.757)
Ti	(0 0 0.008)	(0 0 0)
	(0 0 0.503)	(0 0 0.500)
O	(-0.338 -0.101 0.567)	(-0.336 -0.126 0.577)
	(-0.233 -0.333 0.405)	(-0.207 -0.330 0.410)
Monoclinic phase		
	<i>Calc.</i>	<i>Ref. [21]</i>
<i>a</i>	9.555	9.526
<i>b</i>	5.508	5.483
<i>c</i>	5.634	5.507
α	90°	90°
β	125.742°	125.344°
Na	(0.502 0.750 -0.006)	(0.500 0.750 0)
Bi	(-0.003 0.256 0.036)	(0 0.250 0)
Ti	(0.255 0.243 0.744)	(0.270 0.247 0.742)
O	(-0.014 0.180 0.414)	(0.008 0.194 0.493)
	(0.189 0.486 0.901)	(0.177 0.481 0.862)
	(0.262 0.981 0.951)	(0.241 0.996 0.955)
Tetragonal phase		
	<i>Calc.</i>	<i>Ref. [7]</i>
<i>a</i>	5.410	5.519
<i>c</i>	7.925	7.817
α	90°	90°
Na	(0 0.5 0.253)	(0 0.5 0.261)
Bi	(0 0.5 0.759)	(0 0.5 0.761)
Ti	(0 0 0.019)	(0 0 0)
O	(0 0 0.259)	(0 0 0.257)
	(0 0 0.761)	(0 0 0.757)
Cubic phase		
	<i>Calc.</i>	<i>Ref. [19]</i>
<i>a</i>	7.765	7.827
α	90°	90°
Na	(0 0 0)	(0 0 0)
Bi	(0.5 0.5 0.5)	(0.5 0.5 0.5)
Ti	(0.25 0.25 0.25)	(0.25 0.25 0.25)
O	(0.25 0.25 0)	(0.25 0.25 0)

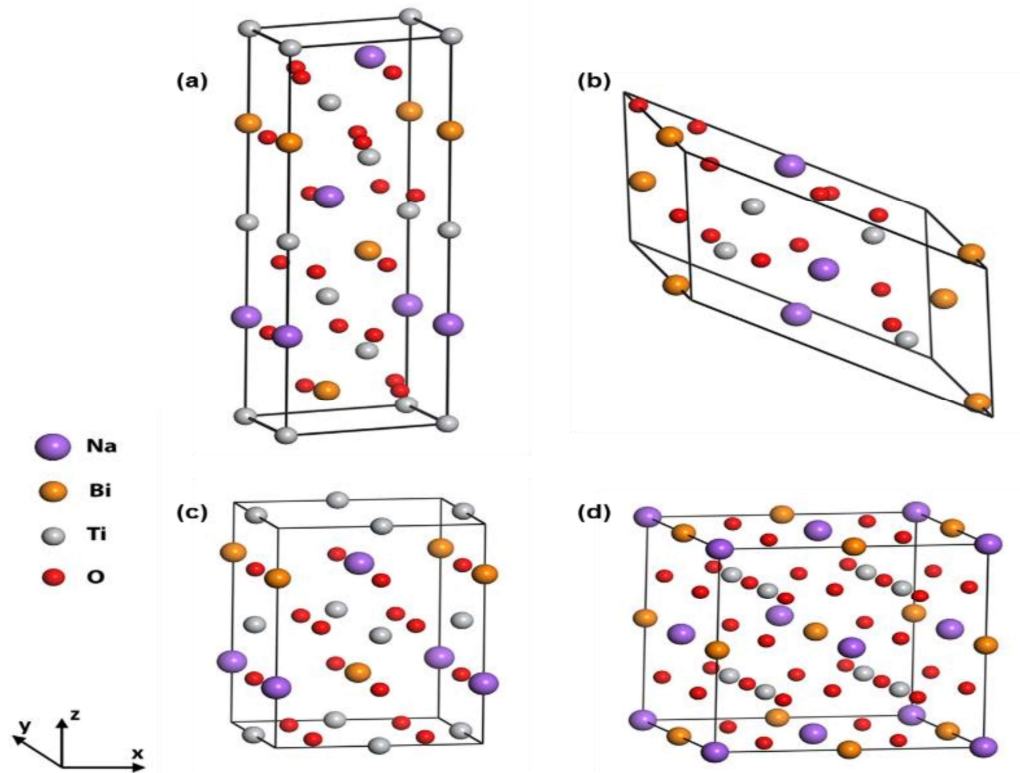


Figure 1. Crystal structures of (a) rhombohedral, (b) monoclinic, (c) tetragonal, and (d) cubic phase of BNT

The corresponding atomic coordinates are also given for the four BNT phases in Table 1. Atoms in rhombohedral and monoclinic phases are imposed by the symmetries of space groups $R3c$ and Cc , respectively, where the symmetries allow them to be relaxed separately. In contrast, atoms in the tetragonal and cubic phases of BNT have higher symmetry structures. Ti atom of the cubic phase has six nearest O atoms, and Na or Bi atom has twelve nearest O atoms. Thus, Ti atoms are in the center of oxygen-octahedral and Na, or Bi is in the center of oxygen-cuboctahedral [19]. From the cubic phase, the displacements of Na, Bi, and Ti atoms with respect to the center of the O cages are calculated for the tetragonal phase. In addition, Na and Bi atoms in the rhombohedral and monoclinic phases have been arranged into layer-by-layer, being favorable conditions for supercell calculations.

3.2. Electronic structures

There is some disparity between different calculations on the band structure of BNT. For the rhombohedral phase, H. Lü [19] gave an indirect bandgap of 2.82 eV, while R. Bujakiewicz-Koronska [13] predicted a value of about 2 eV. For the tetragonal and cubic phases, H. Lü [19] gave a bandgap of 2.29 eV and 1.96 eV, respectively. As this work results are shown in Fig.2, the rhombohedral phase has a direct bandgap of 2.764 eV, while the monoclinic phase, tetragonal phase, and cubic phase have indirect bandgaps of 2.575

eV, 2.189 eV, and 1.473 eV, respectively. For the rhombohedral, monoclinic, and cubic phases, the top of the valence band is located at the G(0 0 0) point. The bottom of the conduction band for the rhombohedral phase is also located at the G point, while for the monoclinic and cubic phases, it is at the B and R points, respectively. The direct bandgaps were estimated at 2.764 eV, 2.580 eV, 2.192 eV, and 2.150 eV for rhombohedral, monoclinic, tetragonal, and cubic BNT materials, respectively. Overall, the bandgap values of the four BNT phases indicate that they are suitable optical materials.

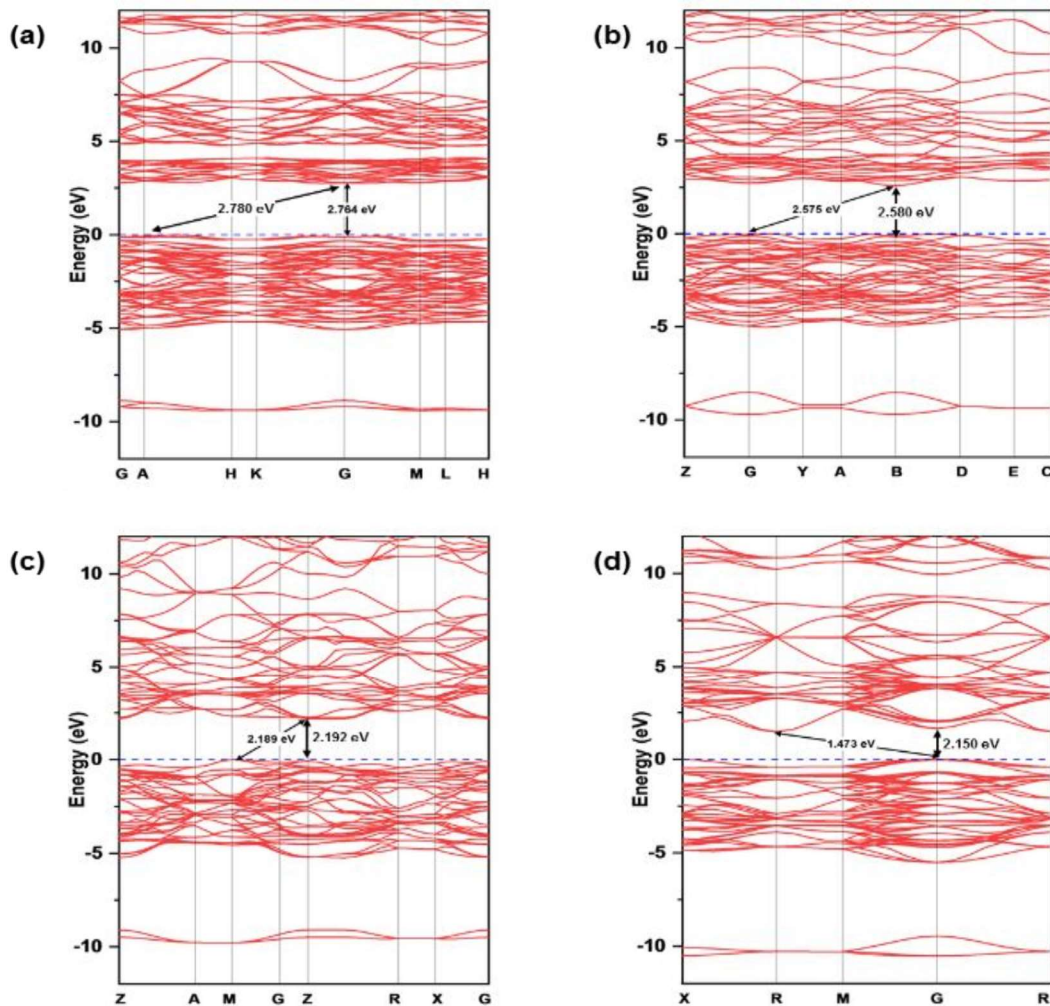


Figure 2. Band structures of (a) rhombohedral, (b) monoclinic, (c) tetragonal, and (d) cubic BNT phases

Fig.3 shows the contribution of each cation and anion in the calculated partial densities of state (PDOS) of the four BNT phases. In all the cases, the contributions of *p*-orbitals of Bi, *d*-orbitals of Ti, and *p*-orbitals of O are significant within the low energy range. In addition, the hybridization of *d*-orbitals of Ti and *p*-orbitals of O occurs within the low energy range of approximately -6 eV. In the range above Fermi level, the contribution of Ti *d*-orbitals is appeared to create a boundary of the bandgap; Bi *p*-orbitals also contributed to this range. Still, it is the only evidence in the high-temperature phases.

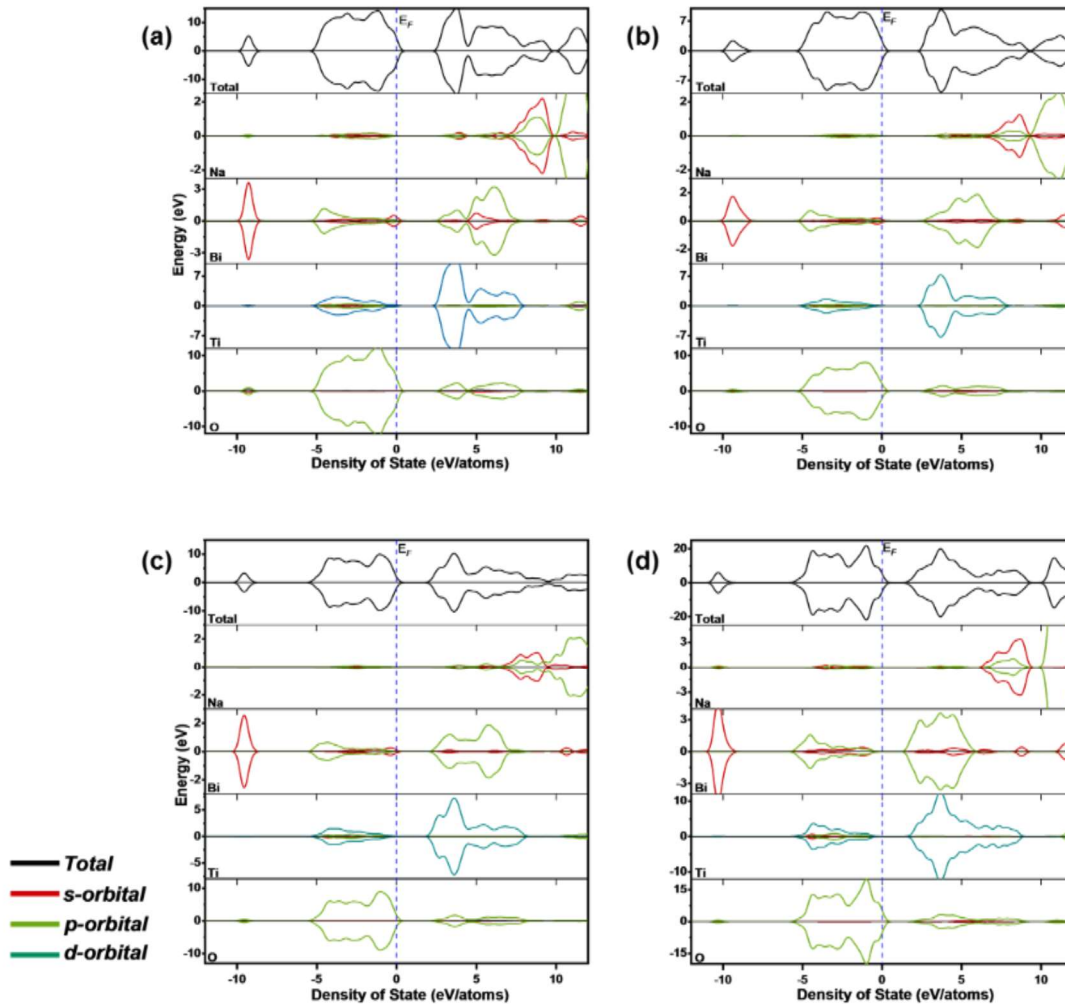


Figure 3. The densities of state of (a) rhombohedral, (b) monoclinic, (c) tetragonal, and (d) cubic phase of BNT

4. Conclusion

We have studied the structural and electronic properties of ($-\text{Bi}_{0.5}\text{Na}_{0.5}\text{TiO}_3-$) materials in four possible phases using first-principle calculations. The equilibrium structures were determined, and the contributions of p -orbitals of Bi and O, and Ti d -orbitals are significant within the low energy range. The contribution of d -orbitals of Ti is essential creating the bandgap, and p -orbitals of Bi are also crucial in the high symmetry phases. The direct bandgap of 2.76 eV and indirect bandgap of 1.5~2.6 eV for the rhombohedral and higher symmetry phases, respectively. Thus, BNT materials have good potential in optical materials. Furthermore, we expected that our works could help to understand the role of phase transition in lead-free ferroelectric sodium bismuth titanate materials.

Acknowledgments: We would like to acknowledge the financial support from The Ministry of Science and Technology, Viet Nam, under project number DTĐLCN.29/18.

References

- [1] N. D. Quan, L. H. Bac, D. V. Thiet, V. N. Hung, and D. D. Dung (2014), Current development in lead-free $\text{Bi}_{0.5}(\text{Na,K})_{0.5}\text{TiO}_3$ -based piezoelectric materials, *Adv. Mater. Sci. Eng.* 365391. <https://doi.org/10.1155/2014/365391>.
- [2] D. D. Dung, N. T. Hung, D. Odkhuu (2020), Structure, optical and magnetic properties of new $\text{Bi}_{0.5}\text{Na}_{0.5}\text{TiO}_3$ - $\text{SrMnO}_{3-\delta}$ solid solution materials. *Sci. Rep.* 9, 18186. <https://doi.org/10.1038/s41598-019-54172-4>.
- [3] T. Takenaka, K. I. Maruyama, K. Sakata (1991), $(\text{Bi}_{1/2}\text{Na}_{1/2})\text{TiO}_3$ - BaTiO_3 System for Lead-Free Piezoelectric Ceramics, *Japanese J. Appl. Phys.* 30, 2236-2239. <https://doi.org/10.1143/JJAP.30.2236>.
- [4] G. O. Jones, P. A. Thomas (2020), Investigation of the structure and phase transitions in the novel A-site substituted distorted perovskite compound $\text{Na}_{0.5}\text{Bi}_{0.5}\text{TiO}_3$, *Acta Crystallogr B* 58, 168-178, <https://doi.org/10.1107/S0108768101020845>.
- [5] E. Aksel, J. S. Forrester, J. L. Jones, P. A. Thomas, K. Page, M. R. Suchomel (2011), Monoclinic crystal structure of polycrystalline $\text{Na}_{0.5}\text{Bi}_{0.5}\text{TiO}_3$, *Appl. Phys. Lett.* 98 152901. <https://doi.org/10.1063/1.3573826>.
- [6] I. P. Pronin, P. P. Syrnikov, V. A. Isupov, V. M. Egorov, N. V. Zaitseva, A. F. Ioffe (1980), Peculiarities of phase transitions in sodium-bismuth, *Ferroelectrics*, 25, 395-397. <https://doi.org/10.1080/00150198008207029>.
- [7] G. O. Jones, P. A. Thomas (2020), The tetragonal phase of $\text{Na}_{0.5}\text{Bi}_{0.5}\text{TiO}_3$ - a new variant of the perovskite structure, *Acta Cryst. B*, 56, 426-430. <https://doi.org/10.1107/S0108768100001166>
- [8] S. Kuharunggrong, W. Schulze (1996), Characterization of $\text{Bi}_{0.5}\text{Na}_{0.5}\text{TiO}_3$ - PbTiO_3 M Dielectric Materials, *J. Am. Ceram. Soc.* 79, 1273. <https://doi.org/10.1111/j.1151-2916.1996.tb08584.x>.
- [9] S. E. Park, S. J. Chung, I. T. Kim (1996), Ferroic Phase Transitions in $(\text{Na}_{1/2}\text{Bi}_{1/2})\text{TiO}_3$ Crystals, *J. Am. Ceram. Soc.* 79, 1290. <https://doi.org/10.1111/j.1151-2916.1996.tb08586.x>
- [10] J. Suchanicz, W. S. Ptak (1990), On the phase transition in $\text{Na}_{0.5}\text{Bi}_{0.5}\text{TiO}_3$, *Ferroelectr., Lett. Sect.* 12, 71. <https://doi.org/10.1080/07315179008201119>.
- [11] W. H. Duan, Z. R. Liu (2006), Theoretical modeling and simulations of perovskite ferroelectrics: From phenomenological approaches to ab initio, *Curr. Opin. Solid State Mater. Sci.* 10, 40. <https://doi.org/10.1016/j.cossms.2006.06.002>.
- [12] Y. N. Xu, W. Y. Ching (2000), Electronic structure of $(\text{Na}_{1/2}\text{Bi}_{1/2})\text{TiO}_3$ and its solid solution with BaTiO_3 , *Philos. Mag. B* 80, 1141. <https://doi.org/10.1080/13642810008208587>.
- [13] R. B. Koronska, Y. Natanzon (2008), Determination of elastic constants of $\text{Na}_{0.5}\text{Bi}_{0.5}\text{TiO}_3$ from ab initio calculations, *Phase Trans.* 81, 1117. <https://doi.org/10.1080/01411590802460833>.

- [14] M. Gröting, I. Kornev, B. Dkhil, K. Albe (2012), Pressure-induced phase transitions and structure of chemically ordered nanoregions in the lead-free relaxor ferroelectric $\text{Na}_{1/2}\text{Bi}_{1/2}\text{TiO}_3$, *Phys. Rev. B* 86, 134118. <https://doi.org/10.1103/PhysRevB.86.134118>.
- [15] M. K. Niranjana, T. Karthik, S. Asthana, J. Pan, U. V. Waghmare (2013), Theoretical and experimental investigation of Raman modes, ferroelectric and dielectric properties of relaxor $\text{Na}_{0.5}\text{Bi}_{0.5}\text{TiO}_3$, *J. Appl. Phys.* 113, 194106. <https://doi.org/10.1063/1.4804940>.
- [16] J.P. Perdew, K. Burke, M. Ernzerhof (1996), Generalized Gradient Approximation Made Simple, *Phys. Rev. Lett.* 77, 3865-3868. <https://doi.org/10.1103/PhysRevLett.77.3865>.
- [17] S. Berri (2018), Ab initio study of fundamental properties of XAlO_3 (X = Cs, Rb and K) compounds, *J. Sci. Adv. Mater. Dev.* 3, 254-261. <https://doi.org/10.1016/j.jsamd.2018.03.001>
- [18] H. J. Monkhorst, J. D. Pack (1976), Special points for Brillouin-zone integrations, *Phys. Rev. B* 13, 5188. <https://doi.org/10.1103/PhysRevB.13.5188>.
- [19] H. Lü, S. Wang, X. Wang (2014), The electronic properties and lattice dynamics of $(\text{Na}_{0.5}\text{Bi}_{0.5})\text{TiO}_3$: From cubic to tetragonal and rhombohedral phases, *J. Appl. Phys.* 115, 124107. <https://doi.org/10.1063/1.4869733>.
- [20] S. Takagi, A. Subedi, V. R. Cooper, D. J. Singh (2010), Effect of A-site size difference on polar behavior in M BiScNbO_6 (M=Na, K, and Rb): Density functional calculations, *Phys. Rev. B* 82, 134108. <https://doi.org/10.1103/PhysRevB.82.134108>.
- [21] E. Aksel, J. S. Forrester, J. L. Jones, P. A. Thomas, K. Page, M. R. Suchomel (2011), Monoclinic crystal structure of polycrystalline $\text{Na}_{0.5}\text{Bi}_{0.5}\text{TiO}_3$, *Appl. Phys. Lett.* 98, 152901. <https://doi.org/10.1063/1.3573826>.

INTEGRATED RESOLVENT OPERATORS AND NONDENSELY INTEGRODIFFERENTIAL EQUATIONS INVOLVING THE NONLOCAL CONDITIONS

Hoang Thi Lan¹, Le Anh Minh²

Abstract: *The aim of this work is to prove some results of the existence and regularity of solutions for some nondensely integrodifferential equations with nonlocal conditions, where the linear part has an integrated resolvent operator in the sens given by Oka [7]. They extend the results of [4] and [5].*

Keywords: *Integrated resolvent operator, resolvent operator, integral solution, nonlocal, nondensely, integrodifferential equations.*

1. Introduction

Nonlocal conditions in dynamical systems play an important role in many physical problems. They have better effects in applications than the classical initial conditions $u(0) = u_0$. See, for example, in [1,2] to determine the unknown physical parameter in some inverse heat condition problems and in [3] to describe the diffusion phenomenon of a small amount of gas in a transparent tube. As indicated in [8], we sometimes need to deal with non-densely defined operators. For example, when we look at a one-dimensional heat equation with Dirichlet conditions on $[0, \pi]$ and consider $A = \frac{\partial^2}{\partial x^2}$ in $C([0, \pi], \mathbb{R})$, in order to measure the solutions in the sup-norm, then the domain.

$$D(A) = \{u \in C^2([0, \pi], \mathbb{R}) : u(0) = u(\pi) = 0\}$$

is not dense in $C([0, \pi], \mathbb{R})$ with the sup-norm since

$$\overline{D(A)} = \{u \in C([0, \pi], \mathbb{R}) : u(0) = u(\pi) = 0\} \neq C([0, \pi], \mathbb{R}).$$

In this work, we are concerned with the existence and regularity of solutions for the following nondensely nonlocal integrodifferential equation

$$u'(t) = Au(t) + \int_0^t B(t-s)u(s)ds + f(t, u(t)) \quad \text{for } t \in [0, a] \tag{1.1}$$

$$u(0) = u_0 + g(u)$$

where $A: D(A) \subset X \rightarrow X$ is a nondensely defined closed linear operator on a Banach space X , $(B(t))_{t \geq 0}$ is a family of closed linear operators on X having the same domain $D(B) \supset D(A)$ which is independent of t , $f: [0, a] \times X \rightarrow X$ and $g: C([0, a]; X) \rightarrow X$ are given functions to be specified later, where $C([0, a]; X)$ denotes the space of continuous function form $[0, a]$ to X .

¹ Bim Son High School, Thanh Hoa Province

² Faculty of Natural Sciences, Hong Duc University; Email: leanhminh@hdu.edu.vn